Surface-Induced Phase Transition of Asymmetric Diblock Copolymer in Selective Solvents

Rong Wang,*,† Zhibin Jiang,† Yeng-Long Chen,‡ and Gi Xue†

Department of Polymer Science and Engineering, School of Chemistry and Chemical Engineering, Nanjing University, Nanjing 210093, People's Republic of China, and Institute of Physics and Research Center for Applied Sciences, Academia Sinica, Taipei, 11529 Taiwan

Received: July 6, 2006; In Final Form: August 31, 2006

Surface-induced phase transition of asymmetric diblock copolymer in selective solvents is first theoretically investigated by using the real-space version of self-consistent field theory (SCFT). By varying the distance between two parallel hard surfaces (or the film thickness) W and the block copolymer concentration f_p, several morphologies are predicted and the phase diagram is constructed. Self-assembly morphologies of the diblock copolymer in dilute solution are found to change significantly with different film thickness. In confined systems, stable morphologies found in the bulk solution become unstable due to the loss of polymer conformation entropy. We find that in a very dilute block copolymer solution, phase separation can be induced through polymer depletion as the solution becomes more confined. Our findings provide an interesting starting point for a renewed effort in both experimental and theoretical investigations of confined block copolymer solutions.

I. Introduction

Self-assembly and phase separation in diblock copolymers have been well-studied and -characterized both theoretically and experimentally in the past few decades.[1−8] Block copolymers can microphase-separate into a wide range of highly ordered nanoscale morphologies for the design of desirable nanomaterials.[9,10] In thin films, incompatibility between different polymer components and the thin film thickness creates frustration, the effect of which can be probed by surface-induced effect. The presence of a surface or interface can strongly influence the microdomain morphologies and the kinetics of microdomain ordering. In general, phase separation is accompanied by a minimization of the interfacial area of contact between dissimilar components, resulting in a reduction of the enthalpy. This is accompanied by a reduction of the conformational entropy of the polymer chains. The complex and rich micromorphologies depend not only on the molecular parameters such as the interaction energies between distinct blocks and the architectures of the block copolymers but also on external variables such as the electric fields,[11,12] the temperature gradients,[13] the chemically patterned substrates,[14−21] and the interfacial interactions.[22−25]

Surface effects play important roles in the solution stability in thin films. The phase behavior of diblock copolymers melts confined in a parallel slit or in a thin film has been extensively studied.[26−32] Much of the current work focuses on the influence of surfaces or interfaces on the ordering properties of symmetric diblock copolymers, $f = 0.5$.[33,34] The lamellae morphology of block copolymers can align either parallel or perpendicular to the surfaces, depending on the film thickness and the wetting properties of the confining surfaces.[35] Asymmetric diblock copolymer films with comparable thickness to the bulk domain also often form the lamellar morphology.[30,31,36] Relatively little work has been done on the phase behavior of thin films of asymmetric block copolymers until recently.[30,31,36]

Asymmetric block copolymers can form vesicles and different micelles such as spherelike and rodlike micelles in selective solvents.[37−41] Among these microstructures, vesicles are of fundamental and practical interests as they have many potential applications as microreactors, microcapsules, and drug delivery systems.[42−44] Solvent-influenced ordering has been exploited to control the morphology of block copolymer thin films without any thermal treatment.[45−50] The adsorption of diblock copolymers from a selective solvent onto a flat solid substrate also results in the formation of laterally ordered microdomains.[51−54]

The morphologies or self-assemblies of the amphiphilic highly asymmetric diblock or triblock copolymer with minor end blocks in dilute solution have been widely studied experimentally[37,38,40,55,56] and even theoretically.[41,57−59] However, there has been little consideration on the self-assemblies of block copolymers in dilute solution in confined systems, which are of interest in many biological systems. The phase behavior of block copolymer in dilute solution may be very different from that in the bulk. A hard surface or interface will induce polymer depletion, which can lead to local concentration gradients and solution phase separation under the appropriate conditions.[60,61]

In this work, we extend theoretical consideration to the surface-induced phase transition of block copolymers in solutions. On the basis of the recent development of self-consistent field theory (SCFT) for the study of morphologies (e.g. two-dimensional circular and linear micelles corresponding to vesicle/spherelike and rodlike micelles in three dimensions) of the amphiphilic block copolymer in dilute solution,[41,57−59,62] we investigate the phase behavior of confined asymmetric diblock copolymers in solution in a parallel slit. The influences of the slit height and the concentration on block copolymer morphology are studied systematically, and the phase diagram is constructed. In the next section we briefly introduce the SCFT formulation used in our study. The results of the calculations and simulations are presented in section III.

II. Theoretical Method

We employ the SCFT for a mixture of n_p linear AB diblock copolymers with n_s solvent molecules confined between two parallel hard surfaces, as shown in Figure 1. Each copolymer chain consists of N segments with compositions (average volume

* To whom correspondence should be addressed. E-mail: rong_wang73@hotmail.com.
† Nanjing University.
‡ Academia Sinica.

10.1021/jp064268+ CCC: $33.50
Published on Web 10/18/2006

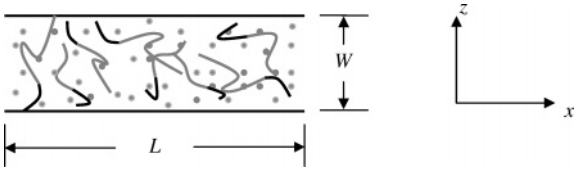

Figure 1. Schematic diagram of AB diblock copolymer solution confined between two parallel hard surfaces. The black, gray lines, and small light gray spheres represent blocks A, B, and solvents, respectively. L and W are the length and thickness of the film, respectively.

fractions) f_A and f_B ($f_B = 1 - f_A$), respectively. We assume the mixture is incompressible, with each polymer segment occupying a fixed volume ρ_0^{-1} and each solvent molecule taking the same volume $\upsilon_S = \rho_0^{-1}$. Thus, the total volume of the system is $V = n_p N/\rho_0 + n_S \upsilon_S$, the volume fraction of the AB diblock copolymer is $f_p = n_p N/V\rho_0$ and that of the solvent is $f_S = 1 - f_p$. Furthermore, we assume that the A and B segments have the same segment length a.

In the SCFT one considers the statistics of a single copolymer chain in a set of effective chemical potential fields w_i, where i represents block species A, B, or solvent S. These chemical potential fields, which represent the actual interactions between different components, are conjugated to the segment density fields, ϕ_i, of different species i. The free energy of the system is given by

$$\frac{NF}{k_B T \rho_0 V} = -f_p \ln(Q_p/f_p V) - N f_S \ln(Q_S/f_S V) - 1/V \int d\mathbf{r}[w_A\phi_A + w_B\phi_B + w_S\phi_S + \xi(1 - \phi_A - \phi_B - \phi_S)] + 1/V \int d\mathbf{r}[\chi_{AB}N\phi_A\phi_B + \chi_{AS}N\phi_A\phi_S + \chi_{BS}N\phi_B\phi_S] \quad (1)$$

where χ_{ij} is the Flory−Huggins interaction parameter between species i and j and ξ is the Lagrange multiplier (which acts as a pressure). $Q_p = \int d\mathbf{r}\, q(\mathbf{r},1)$ is the partition function of a single chain in the effective chemical potential fields w_A and w_B. $Q_S = \int d\mathbf{r} \exp(-w_S(\mathbf{r})/N)$ is the partition function of the solvent in the effective chemical potential field w_S. The fundamental quantity to be calculated in mean-field studies is the chain propagator $q(\mathbf{r},s)$, which represents the probability of finding the end of a segment with contour length s at position r. $q(\mathbf{r},s)$ satisfies a modified diffusion equation using a flexible Gaussian chain model[63]

$$\frac{\partial}{\partial s} q(\mathbf{r},s) = \frac{Na^2}{6}\nabla^2 q(\mathbf{r},s) - w q(\mathbf{r},s) \quad (2)$$

where $w = w_A$ when $0 < s < f_A$ and w_B when $f_A < s < 1$. The initial condition of eq 2 satisfies $q(\mathbf{r},0) = 1$. Because the two ends of the AB block copolymer are different, a second chain propagator $q^+(\mathbf{r},s)$ is needed which satisfies eq 2, with the right-hand side multiplied by -1 and the initial condition $q^+(\mathbf{r},1) = 1$. The density of each component is obtained by

$$\phi_A(\mathbf{r}) = \frac{f_p V}{Q}\int_0^{f_A} ds\, q(\mathbf{r},s)\, q^+(\mathbf{r},s) \quad (3)$$

$$\phi_B(\mathbf{r}) = \frac{f_p V}{Q}\int_{f_A}^{1} ds\, q(\mathbf{r},s)\, q^+(\mathbf{r},s) \quad (4)$$

$$\phi_S(\mathbf{r}) = \frac{f_S V}{Q_S} \exp(-w_S(\mathbf{r})/N) \quad (5)$$

Minimization of the free energy with respect to density and pressure, $\delta F/\delta\phi = \delta F/\delta\xi = 0$, leads to another four equations.

$$w_A(\mathbf{r}) = \chi_{AB}N\phi_B(\mathbf{r}) + \chi_{AS}N\phi_S(\mathbf{r}) + \xi(\mathbf{r}) \quad (6)$$

$$w_B(\mathbf{r}) = \chi_{AB}N\phi_A(\mathbf{r}) + \chi_{BS}N\phi_S(\mathbf{r}) + \xi(\mathbf{r}) \quad (7)$$

$$w_S(\mathbf{r}) = \chi_{AS}N\phi_A(\mathbf{r}) + \chi_{BS}N\phi_B(\mathbf{r}) + \xi(\mathbf{r}) \quad (8)$$

$$\phi_A(\mathbf{r}) + \phi_B(\mathbf{r}) + \phi_S(\mathbf{r}) = 1 \quad (9)$$

We solve eqs 3−9 directly in real space by using a combinatorial screening algorithm proposed by Drolet and Fredrickson.[64,65] The algorithm consists of randomly generating the initial values of the fields $w_i(r)$. Using a Crank−Nicholson scheme and an alternating-direct implicit (ADI) method,[66] the diffusion equations are then integrated to obtain q and q^+, for $0 < s < 1$. Finally, the right-hand sides of eqs 3−5 are evaluated to obtain new values for the volume fractions of blocks A, B, and solvent S.

The numerical calculations were performed in two-dimensional space with $L \times W$ grid points in the xz-plane. The surfaces were represented as lines with a thickness of 1 grid point and positioned at 0 and $W + 1$. The grid size $\Delta x = \Delta z = \Delta = 0.5a$. Periodic boundary is used along the x-direction, and the regions of $z < 1$ and $z > W$ are forbidden. All calculations have been done with $L = 200\Delta$, which is large enough ($L \gg R_g$) to avoid periodic boundary effects on the microstructure. Our simulation is performed using an initial random distribution of concentration with a fluctuation amplitude of $\Delta f_p = 10^{-4}$ to ensure that the observed morphologies are independent of the initial condition. The simulation is carried out until the phase patterns are stable and the free energy difference between two iterations is smaller than 10^{-6}, i.e., $\Delta F < 10^{-6}$. All the simulations are repeated by using different random numbers to guarantee the observed structures are not artifacts.

Our calculations investigate the A_3B_{17} diblock copolymers ($f_A = 0.15$) with a radius of gyration (R_g) of $1.826a$ in selective solvent. The interaction parameters are set to be the following: $\chi_{AB}N = 15$, $\chi_{AS}N = 0.5$, and $\chi_{BS}N = 25$. Therefore, the solvent is a good solvent for block A; i.e., block A is hydrophilic and short enough to ensure the crew-cut aggregates are formed.

III. Results and Discussion

We first discuss how the distance between two hard surfaces affects the block copolymer morphologies. We focus on the block copolymers in dilute and/or semidilute solution because amphiphilic block copolymers can form vesicles and different complex micelles such as spherelike and rodlike micelles.[37−40] By continuously varying the film thickness W and the concentration of block copolymers f_p, we have constructed the phase diagram shown in Figure 2. The lines represent the calculated theoretical phase boundaries. There are at least six phase regions found in our simulation: Dis, V, V + S, V + S + R, R + S, and R, which correspond to the disordered phase; vesicles; mixtures of vesicles and spheres; mixtures of vesicle, spheres, and rods; mixtures of rods and spheres; and rods in 3D, respectively. We will use the 3D descriptions for different morphologies to clearly describe our 2D results.

Vesicles easily form in very dilute block copolymer solution.[37,38,40,55] The stable morphologies formed by the A_3B_{17} diblock copolymers in selective solvents for different film thicknesses at $f_p = 0.15$ are shown in Figure 3. Figure 3a shows that, in bulk solution, the block copolymers form a stable

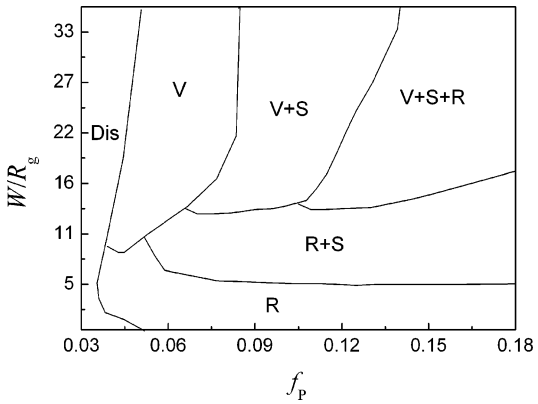

Figure 2. Phase diagram of confined asymmetric diblock copolymer in selective solvents as a function of W and f_p. The parameters are $f_A = 0.15$, $\chi_{AB}N = 15$, $\chi_{AS}N = 0.5$, and $\chi_{BS}N = 25$.

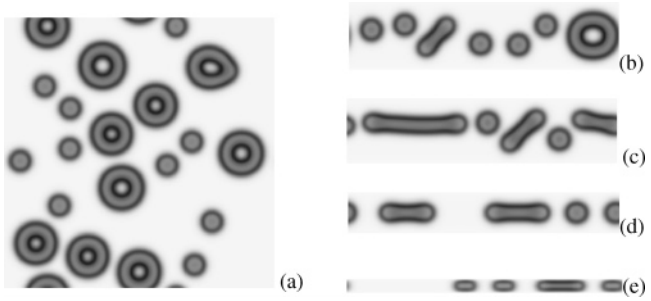

Figure 3. Morphologies of the asymmetric AB diblock copolymers in selective solvent with different film thicknesses at $f_p = 0.15$: (a) stable morphology in bulk system (without confinement), (b) $W = 50\Delta$ ($13.7R_g$), (c) $W = 48\Delta$ ($13R_g$), (d) $W = 30\Delta$ ($8.2R_g$), and (e) $W = 10\Delta$ ($2.7R_g$). The black and gray colors represent blocks A and B, respectively.

mixture of vesicles and spherelike micelles (V + S). The stable morphologies change with confinement. When the hard walls are far from each other, the morphology is similar to the one in bulk. For $W = 50\Delta$ ($13.7R_g$) the number of vesicles decreases and the rodlike micelles emerge, and the solution contains a stable mixture of vesicle, rodlike, and sphere-like micelles (V + S + R), as shown in Figure 3b. As the confinement further decreases to $W = 48\Delta$ ($13R_g$), the vesicles disappear and only rodlike and spherelike micelles remain (R + S), as shown in Figure 3c. The change in the morphologies from $W = 50\Delta$ to $W = 48\Delta$ results from the fact that the spherelike and rodlike micelles are more entropically favorable than the vesicle when the film thickness W is comparable to the diameter of the vesicles. Only the rodlike micelles are found if the confinement is less than four to five times R_g of the diblock copolymer (see Figure 3e). The rodlike micelles align parallel to the surface to avoid frustration and decrease the free energy of the system.

Figure 4 shows the transition between different morphologies of the A_3B_{17} block copolymer under bulk and confined conditions at $f_p = 0.075$. In the bulk, only the vesicle morphology is observed (V). As the confinement strength increases, the spherelike micelles (V + S) appear, as seen in Figure 4b. Vesicle formation is suppressed at $W = 35\Delta$ ($9.6R_g$) for the same reason as for the $f_p = 0.15$ system, and only spherelike and rodlike micelles are found (R + S).

The most interesting observation for the A_3B_{17} block copolymer solution is that phase separation occurs in a confined system when the copolymer solution is so dilute that the solution is well-mixed in the bulk, such as for $f_p = 0.05$. The disordered phase is stable until the starlike aggregates of vesicles form at $W = 130\Delta$. Figure 5 shows the morphologies of the block

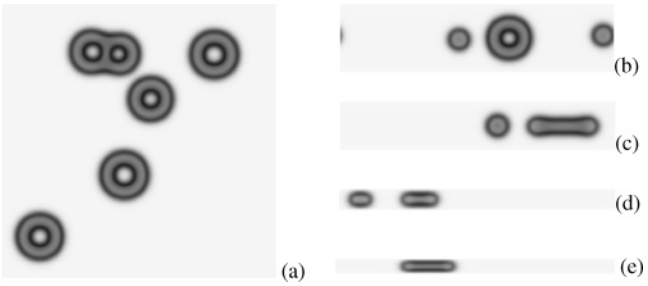

Figure 4. Morphologies of the asymmetric AB diblock copolymers in selective solvent with different thicknesses of the film at $f_p = 0.075$: (a) stable morphology in bulk system (without confinement), (b) $W = 50\Delta$ ($13.7R_g$), (c) $W = 35\Delta$ ($9.6R_g$), (d) $W = 15\Delta$ ($4.1R_g$), and (e) $W = 10\Delta$ ($2.7R_g$).The black and gray colors represent blocks A and B, respectively.

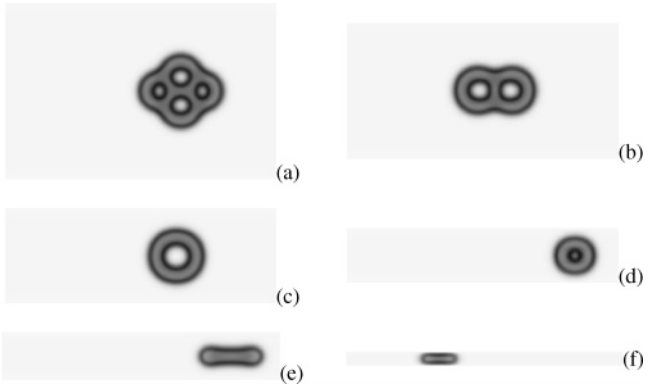

Figure 5. Morphologies of the asymmetric AB diblock copolymers in selective solvent with different thicknesses of the film at $f_p = 0.05$: (a) $W = 130\Delta$ ($35.6R_g$), (b) $W = 100\Delta$ ($27.4R_g$), (c) $W = 70\Delta$ ($19.2R_g$), (d) $W = 40\Delta$ ($11R_g$), (e) $W = 35\Delta$ ($9.6R_g$), and (f) $W = 10\Delta$ ($2.7R_g$). The black and gray colors represent blocks A and B, respectively.

copolymers for $W = 130\Delta$, 100Δ, 70Δ, 40Δ, 35Δ, and 10Δ (35.6, 27.4, 19.2, 11, 9.6, and $2.7R_g$). The aggregate number of vesicles decreases as the confinement increases, and the budding vesicle forms at $W = 100\Delta$ (Figure 5b). Separated vesicles form as we further decrease W to below 70Δ (Figure 5c). In contrast to the $f_p = 0.15$ case in Figure 3c, it is more energetically favorable for the diameter of the vesicle to decrease than form spherelike micelles due to the very dilute block copolymer concentration. The morphology changes from the vesicle morphology directly to the rodlike micelles, without an observation of the spherelike micelles. In this very dilute solution, confinement not only can induce phase transition but it also reduces the morphology space.

To clarify the role of confinement on introducing long-range order of the microdomains, we consider the density profiles of block copolymers perpendicular to the surfaces at film thicknesses in which the solution is disordered. Figure 6 shows the one-dimensional density profiles along the z-direction at $f_p = 0.05$ with $W = 180\Delta$ ($49.3R_g$), 150Δ ($41.1R_g$), and 135Δ ($37R_g$). A depleted region of block copolymers can be clearly seen near the surfaces. Polymer segments are excluded from the surface due to the conformational restrictions, leading to higher concentration of block copolymers at the central part of the film. As the confinement effect increases from $W = 180\Delta$ to 135Δ, the depletion region grows relative to the slit height (but remains approximately R_g), resulting in higher concentration of block copolymers in the center of the film and higher solvent concentration near the surfaces. Moreover, blocks A (hydrophilic) tend to aggregate closer to the surfaces than blocks B (hydrophobic) due to higher solvents concentration near the

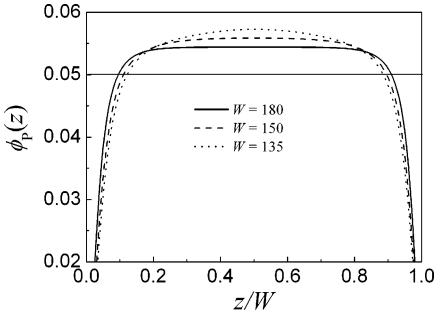

Figure 6. Density profile of diblock copolymers perpendicular to the surfaces at $f_p = 0.05$ with $W = 180\Delta$ ($49.3R_g$) (solid line), 150Δ ($41.1R_g$) (dashed line), and 135Δ ($37R_g$) (dotted line). The abscissa of the figure is reduced by W.

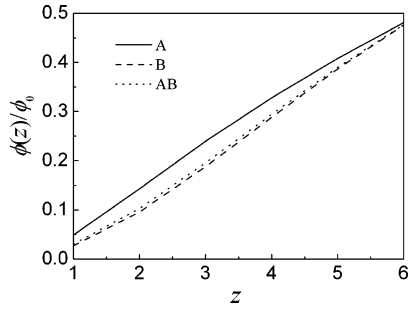

Figure 7. Reduced density profile of diblock copolymers perpendicular to the surfaces at $f_p = 0.05$ with $W = 135\Delta$ ($37R_g$).

surfaces, as shown in Figure 7. The block copolymers self-assemble when the concentration of polymers in the slit center is larger than the critical micelle concentration (cmc $\sim$ 0.058 in the bulk solution in this case).

To elucidate how confinement affects the phase transition of the block copolymer, we provide insight by calculating the entropic contributions from the block copolymer and the solvent, as well as the enthalpy of the interfacial polymer−solvent and different block interactions. The entropy of a single block copolymer chain S/k_B is given by

$$\frac{S}{k_B} = \ln\left(\frac{Q_P}{f_P V}\right) + \frac{1}{f_P V}\int d\mathbf{r}\,(w_A\phi_A + w_B\phi_B) \qquad (10)$$

And the entropy of a single solvent molecule S_S/k_B is

$$\frac{S_S}{k_B} = \ln\left(\frac{Q_S}{f_S V}\right) + \frac{1}{Nf_S V}\int d\mathbf{r}\, w_S\phi_S \qquad (11)$$

The interfacial energy F_{int} is described by

$$\frac{NF_{int}}{k_B T\rho_0 V} = \frac{1}{V}\int d\mathbf{r}\,(\chi_{AB}N\phi_A\phi_B + \chi_{AS}N\phi_A\phi_S + \chi_{BS}N\phi_B\phi_S) - F_{int}{}^0 \qquad (12)$$

where $F_{int}{}^0$ is the reference interaction energy, which takes the form $F_{int}{}^0 = \chi_{AB}Nf_P{}^2f_Af_B + \chi_{AS}Nf_Pf_Af_S + \chi_{BS}Nf_Pf_Bf_S$.

It is well-known that the entropic polymer depletion effect affects the system phase behavior more strongly in dilute and semidilute solutions rather than in concentrated solutions.[61] Figure 8a shows the order−disorder transition of the block copolymer for $f_p = 0.05$ at $W = 130\Delta$ ($\sim 35.6R_g$) and a corresponding sharp decrease in S/k_B. In this case, the decrease in polymer entropy is due to self-assembly of the block copolymer, which is induced by the polymer depletion effect. As shown in Figure 6, the polymer concentration near the center of the confinement is greater than the critical micelle concentration, leading to the self-assembly of vesicle aggregates. As the confinement decreases further, the entropy of a single block copolymer chain S/k_B decreases with decreasing W, and very rapid decrease occurs at a film thickness of approximately 2$\sim$3 R_g. In such highly confined system, vesicles cannot remain stable due to the polymer conformational entropy loss, leading to the rodlike micelle morphology.

The entropy of a single solvent molecule S_S/k_B, in contrast to the polymer entropy, stays almost constant for varying slit

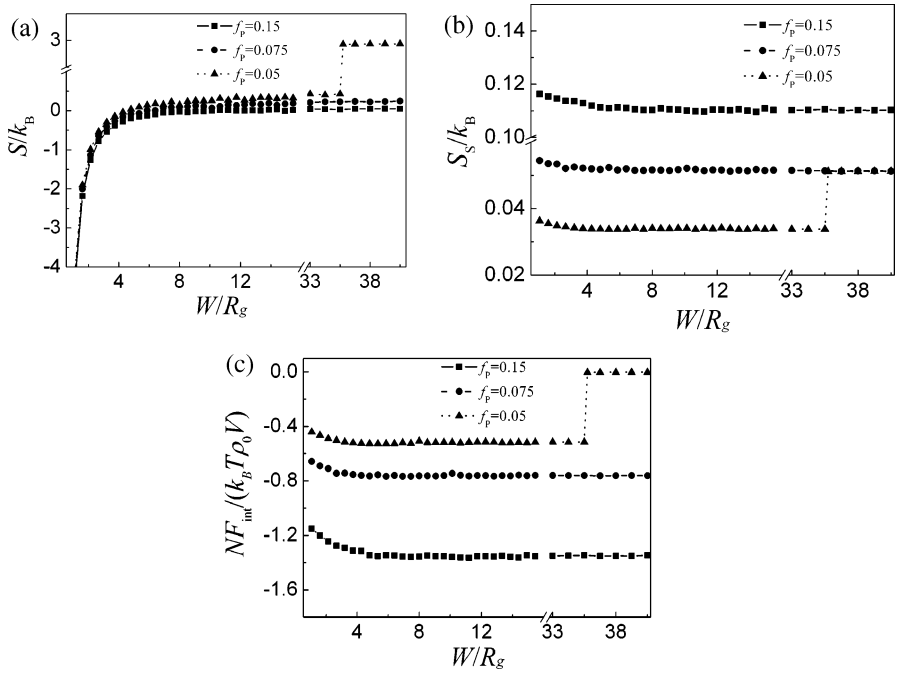

Figure 8. (a) Entropy of a single-block copolymer chain S/k_B, (b) entropy of a single solvent molecule S_S/k_B, and (c) interfacial energy $NF_{int}/(k_BT\rho_0V)$ as a function of the film thickness W for $f_p = 0.15$ (squares), 0.075 (spheres), and 0.05 (triangles).

height through different block copolymer morphologies, as shown in Figure 8b. S_S/k_B changes weakly only when $W \leq 5R_g$, and the depletion of polymers from the walls leads to higher local concentration of solvent molecules near the walls. The interfacial energy change shown in Figure 8c has a trend similar to the entropic free energy of the block copolymers; i.e., the rapid decrease occurs for $W < (2-3)R_g$. Comparing the magnitude of the polymer entropy change, the solvent entropy change, and the interfacial free energy change as the film thickness decreases, the change in the conformation entropy of the block copolymer is the dominant contribution that favors the rod micelle morphology for highly confined systems.

IV. Summary and Conclusion

Confinement-induced phase transition of asymmetric diblock copolymer in selective solvents is investigated by using the real space version of self-consistent field theory (SCFT) for the first time. By varying the film thickness and the concentration of block copolymers, several phases are predicted. The influences of the film thickness and the concentration of block copolymers on chain conformations and interfacial free energy are studied systematically. The predictions show that increasing the confinement effect/reducing the film thickness has a strong influence on the morphologies of the block copolymer in selective solvents. At the highest polymer concentration $f_p = 0.15$, as the slit height decreases from $W = 50\Delta$ to 10Δ, the morphologies change from V + S to V + S + R to R + S and finally to R. At $f_p = 0.075$, the morphology varies from V to V + S to R + S and finally to R. At $f_p = 0.05$, vesicle self-assembly can be induced by confinement as the slit height decreases to $W = 130\Delta$, and the morphology varies from V to R at $W = 35\Delta$. These studies show that the block copolymer concentration also strongly affects the confinement-induced phase transition of block copolymers in solutions.

A very interesting observation is that even for confinement that is much larger than the chain radius of gyration ($W \sim 35.6R_g$), confinement effect alone can induce a phase separation when the copolymer concentration is just below the critical micelle concentration. Polymer depletion can clearly be seen near the surfaces, leading to higher concentration of block copolymers at the central part of the film that is above the cmc. In a highly confined solution ($W \sim (2-3)R_g$), the entropy of the block copolymer dominates the change in micelle morphology because polymer chain conformations are restricted. The change in polymer conformation leads to the reduction of the morphology space, such that strong surface confinement can speed up rearrangement of the microdomains.

The 2D calculation also provides us with a qualitative understanding of the depletion-induced phase transition and morphology changes in the 3D system as the block copolymer solution becomes more confined. For the 3D system, more self-assembled morphologies are possible with the additional degree of freedom. As the polymer depletion effect and the polymer conformational entropy become significantly affected by the confinement, we expect to find changes similar to 2D in the block copolymer morphology. Our findings offer an interesting starting point and a priori knowledge for a renewed effort in both experimental and theoretical investigations of dilute asymmetric block copolymer solutions in confinement. The surface−polymer interactions will strongly affect the phase transition of block copolymers in solutions and will be considered in our following work.

Acknowledgment. This work has been supported by the National Natural Science Foundations of China (Grant Nos. 20504013, 20674035 and 50533020), the Nanjing University Talent Development Foundation (Grant No. 0205004107), and the Natural Science Foundation of Nanjing University (Grant No. 0205005216).

References and Notes

(1) Matsen, M. W.; Schick, M. *Phys. Rev. Lett.* **1994**, *72*, 2660.
(2) Jiang, Y.; Huang, R.; Liang, H. J. *J. Chem. Phys.* **2005**, *123*, 124906.
(3) Srinivas, G.; Discher, D. E.; Klein, M. L. *Nat. Mater.* **2004**, *3*, 638.
(4) Srinivas, G.; Shelley, J. C.; Nielsen, S. O.; Discher, D. E.; Klein, M. L. *J. Phys. Chem. B* **2004**, *108*, 8153.
(5) Glass, R.; Moller, M.; Spatz, J. P. *Nanotechnology* **2003**, *14*, 1153.
(6) Sun, P. C.; Yin, Y. H.; Li, B. H.; Jin, Q. H.; Ding, D. T. *Int. J. Mod. Phys. B* **2003**, *17*, 241.
(7) He, X. H.; Song, M.; Liang, H. J.; Pan, C. Y. *J. Chem. Phys.* **2001**, *114*, 10510.
(8) Muthukumar, M. *Curr. Opin. Colloid Interface Sci.* **1998**, *3*, 48.
(9) Hamley, I. W. *The Physics of Block Copolymers*; Oxford University Press: New York, 1998.
(10) Hamley, I. W. *Nanotechnology* **2003**, *14*, R39.
(11) Morkved, T. L.; Lu, M.; Urbas, A. M.; Ehrichs, E. E.; Jaeger, H. M.; Mansky, P.; Russell, T. P. *Science* **1996**, *273*, 931.
(12) Boker, A.; Elbs, H.; Hansel, H.; Knoll, A.; Ludwigs, S.; Zettl, H.; Urban, V.; Abetz, V.; Muller, A. H. E.; Krausch, G. *Phys. Rev. Lett.* **2002**, *89*, 135502.
(13) van der Meer, P. R.; Meijer, G. C. M.; Vellekoop, M. J.; Kerkvliet, H. M. M.; van den Boom, T. J. J. *Sens. Actuators, A* **1998**, *71*, 27.
(14) Wolff, M.; Scholz, U.; Hock, R.; Magerl, A.; Leiner, V.; Zabel, H. *Phys. Rev. Lett.* **2004**, *92*, 255501.
(15) Ionov, L.; Minko, S.; Stamm, M.; Gohy, J. F.; Jerome, R.; Scholl, A. *J. Am. Chem. Soc.* **2003**, *125*, 8302.
(16) Tsori, Y.; Andelman, D. *Macromolecules* **2001**, *34*, 2719.
(17) Harrison, C.; Adamson, D. H.; Cheng, Z. D.; Sebastian, J. M.; Sethuraman, S.; Huse, D. A.; Register, R. A.; Chaikin, P. M. *Science* **2000**, *290*, 1558.
(18) Pereira, G. G.; Williams, D. R. M. *Langmuir* **1999**, *15*, 2125.
(19) Pereira, G. G.; Williams, D. R. M. *Macromolecules* **1998**, *31*, 5904.
(20) Pereira, G. G.; Williams, D. R. M. *Phys. Rev. Lett.* **1998**, *80*, 2849.
(21) Fasolka, M. J.; Harris, D. J.; Mayes, A. M.; Yoon, M.; Mochrie, S. G. J. *Phys. Rev. Lett.* **1997**, *79*, 3018.
(22) Luzinov, I.; Minko, S.; Tsukruk, V. V. *Prog. Polym. Sci.* **2004**, *29*, 635.
(23) Peters, R. D.; Yang, X. M.; Nealey, P. F. *Macromolecules* **2002**, *35*, 1822.
(24) Walton, D. G.; Soo, P. P.; Mayes, A. M.; Allgor, S. J. S.; Fujii, J. T.; Griffith, L. G.; Ankner, J. F.; Kaiser, H.; Johansson, J.; Smith, G. D.; Barker, J. G.; Satija, S. K. *Macromolecules* **1997**, *30*, 6947.
(25) Mansky, P.; Russell, T. P.; Hawker, C. J.; Mays, J.; Cook, D. C.; Satija, S. K. *Phys. Rev. Lett.* **1997**, *79*, 237.
(26) Matsen, M. W. *J. Chem. Phys.* **1997**, *106*, 7781.
(27) Morkved, T. L.; Jaeger, H. M. *Europhys. Lett.* **1997**, *40*, 643.
(28) Geisinger, T.; Muller, M.; Binder, K. *J. Chem. Phys.* **1999**, *111*, 5241.
(29) Geisinger, T.; Muller, M.; Binder, K. *J. Chem. Phys.* **1999**, *111*, 5251.
(30) Huinink, H. P.; Brokken-Zijp, J. C. M.; van Dijk, M. A.; Sevink, G. J. A. *J. Chem. Phys.* **2000**, *112*, 2452.
(31) Huinink, H. P.; van Dijk, M. A.; Brokken-Zijp, J. C. M.; Sevink, G. J. A. *Macromolecules* **2001**, *34*, 5325.
(32) Rasmussen, K. O. *J. Polym. Sci., Part B: Polym. Phys.* **2004**, *42*, 3695.
(33) Matsen, M. W. *Curr. Opin. Colloid Interface Sci.* **1998**, *3*, 40.
(34) Binder, K. Polymers in Confined Environments. *Adv. Polym. Sci.* **1999**, *138*, 1−89.
(35) Wang, Q.; Nealey, P. F.; de Pablo, J. J. *Macromolecules* **2003**, *36*, 1731.
(36) Yang, Y. Z.; Qiu, F.; Zhang, H. D.; Yang, Y. L. *Polymer* **2006**, *47*, 2205.
(37) Yu, K.; Eisenberg, A. *Macromolecules* **1998**, *31*, 3509.
(38) Burke, S.; Shen, H. W.; Eisenberg, A. *Macromol Symp.* **2001**, *175*, 273.
(39) Zhang, L. F.; Eisenberg, A. *Macromolecules* **1996**, *29*, 8805.
(40) Luo, L. B.; Eisenberg, A. *J. Am. Chem. Soc.* **2001**, *123*, 1012.
(41) Wang, R.; Tang, P.; Qiu, F.; Yang, Y. L. *J. Phys. Chem. B* **2005**, *109*, 17120.
(42) Allen, C.; Maysinger, D.; Eisenberg, A. *Colloids Surf., B* **1999**, *16*, 3.
(43) Gao, Z. S.; Eisenberg, A. *Macromolecules* **1993**, *26*, 7353.
(44) Discher, D. E.; Eisenberg, A. *Science* **2002**, *297*, 967.

(45) Kim, S. H.; Misner, M. J.; Russell, T. P. *Adv. Mater.* **2004**, *16*, 2119.
(46) Kim, S. H.; Misner, M. J.; Xu, T.; Kimura, M.; Russell, T. P. *Adv. Mater.* **2004**, *16*, 226.
(47) Elbs, H.; Drummer, C.; Abetz, V.; Krausch, G. *Macromolecules* **2002**, *35*, 5570.
(48) Fukunaga, K.; Elbs, H.; Magerle, R.; Krausch, G. *Macromolecules* **2000**, *33*, 947.
(49) Kim, G.; Libera, M. *Macromolecules* **1998**, *31*, 2569.
(50) Chen, Y. Z.; Wang, Z. B.; Gong, Y. M.; Huang, H. Y.; He, T. B. *J. Phys. Chem. B* **2006**, *110*, 1647.
(51) Spatz, J. P.; Roescher, A.; Sheiko, S.; Krausch, G.; Moller, M. *Adv. Mater.* **1995**, *7*, 731.
(52) Li, Z.; Zhao, W.; Rafailovich, M. H.; Sokolov, J.; Khougaz, K.; Lennox, B.; Eisenberg, A.; Krausch, G. *J. Am. Chem. Soc.* **1996**, *118*, 10892.
(53) Sohn, B. H.; Yoo, S. I.; Seo, B. W.; Yun, S. H.; Park, S. M. *J. Am. Chem. Soc.* **2001**, *123*, 12734.
(54) Meiners, J. C.; Elbs, H.; Ritzi, A.; Mlynek, J.; Krausch, G. *J. Appl. Phys.* **1996**, *80*, 2224.
(55) Yu, G.; Eisenberg, A. *Macromolecules* **1998**, *31*, 5546.
(56) Liu, F. T.; Eisenberg, A. *J. Am. Chem. Soc.* **2003**, *125*, 15059.
(57) He, X. H.; Liang, H. J.; Huang, L.; Pan, C. Y. *J. Phys. Chem. B* **2004**, *108*, 1931.
(58) Zhu, J. T.; Jiang, Y.; Liang, H. J.; Jiang, W. *J.Phys. Chem. B* **2005**, *109*, 8619.
(59) Li, X.; Tang, P.; Qiu, F.; Zhang, H. D.; Yang, Y. L. *J. Phys. Chem. B* **2006**, *110*, 2024.
(60) Tuinier, R.; Rieger, J.; de Kruif, C. G. *Adv. Colloid Interface Sci.* **2003**, *103*, 1.
(61) Hu, J. L.; Wang, R.; Xue, G. *J. Phys. Chem. B* **2006**, *110*, 1872.
(62) Jiang, Y.; Chen, T.; Ye, F. W.; Liang, H. J.; Shi, A. C. *Macromolecules* **2005**, *38*, 6710.
(63) Helfand, E. *J. Chem. Phys.* **1975**, *62*, 999.
(64) Drolet, F.; Fredrickson, G. H. *Phys. Rev. Lett.* **1999**, *83*, 4317.
(65) Drolet, F.; Fredrickson, G. H. *Macromolecules* **2001**, *34*, 5317.
(66) Press, W. H.; Flannery, B. P.; Teukolsky, S. A.; Vettering, W. T. *Numerical Recipes*; Cambridge Univeristy Press: Cambridge, England, 1989.